Possible second-order nonlinear interactions of plane waves in an elastic solid

V. A. Korneev[a)]
Lawrence Berkeley National Laboratory, Berkeley, California 94720

A. Demčenko
Faculty of Engineering Technology, University of Twente, 7500AE, Enschede, The Netherlands

(Received 21 February 2013; revised 30 October 2013; accepted 9 December 2013)

There exist ten possible nonlinear elastic wave interactions for an isotropic solid described by three constants of the third order. All other possible interactions out of 54 combinations (triplets) of interacting and resulting waves are prohibited, because of restrictions of various kinds. The considered waves include longitudinal and two shear waves polarized in the interacting plane and orthogonal to it. The amplitudes of scattered waves have simple analytical forms, which can be used for experimental setup and design. The analytic results are verified by comparison with numerical solutions of initial equations. Amplitude coefficients for all ten interactions are computed as functions of frequency for polyvinyl chloride, together with interaction and scattering angles. The nonlinear equation of motion is put into a general vector form and can be used for any coordinate system.
[http://dx.doi.org/10.1121/1.4861241]

PACS number(s): 43.25.Lj, 43.25.Jh, 43.25.Dc [MDV] Pages: 591–598

I. INTRODUCTION

Nonlinearity is defined as any deviation from the linear law regarding the transformation of an input signal, due to its propagation through a carrying system. Nonlinearity may appear in a signal at any stage: at elastic wave excitation, at wave propagation through elastic material, through a registration device, or also at the stage of numerical data processing. Here we consider nonlinearity arising as a result of the properties inherent in elastic material. Elastic nonlinearity of different materials, including rock samples, has been observed for ultrasonic frequencies by many authors.[1–9] In particular, it has been shown that the velocity of elastic waves changes with static deformation and hydrostatic pressure. This phenomenon, known as acousto-elasticity, is widely used for measurements of third-order elastic constants in solids. Waves of mixed frequencies as a result of nonlinear wave interaction have also been reported.[10–17] The fundamental equations of nonlinear elastic theory, by Murnaghan,[18] effectively describe such classical nonlinear phenomena as harmonics generation and resonant wave scattering.

The results of this theory are well known among solid state physicists, but most of the information is scattered. Probably the most comprehensive description of the theory can be found in a monograph by Zarembo and Krasil'nikov[19] published in Russian. All possible nonlinear interactions were subsequently presented in a report by Korneev *et al.*[20] In response to the recent growing interest in this subject and a new way of ultrasonic measurements using nonlinear interactions,[16,17] we reconsidered the subject of nonlinear interactions, put them in a more general analytical form and carefully rederived scattering coefficients because in the previous publications their expressions contain some typos and errors. The basic nonlinear equations are put in a vector form, which makes them easy to use in an arbitrary coordinate system. Besides basic equations, this paper presents analytical solutions for all possible nonlinear interactions of collimated beams in a volume of nonlinear elastic material. These solutions are used in Ref. 17 for laboratory observations of material nonlinearity, for nondestructive evaluation and testing purposes.

II. EQUATIONS OF MOTION

The simplest extension of linear dynamic elasticity to a nonlinear (isotropic) form requires addition of three third order elastic (TOE) constants—l, n, and m (Murnaghan notation[18])—in addition to Lamé parameters λ and μ. However, in most previous publications, investigators have used other sets of nonlinear parameters A, B, and C after Landau and Lifschitz,[21] which have simple relations with the previous set,

$$A = n, \quad B = m - n/2, \quad C = l - m + n/2. \tag{1}$$

Assuming elastic deformation in a solid, and that the displacement vector

$$\begin{aligned}\mathbf{u} &= \mathbf{u}(x, y, z) = \mathbf{u}(x_1, x_2, x_3)\\ &= (u_1(x_1, x_2, x_3), u_2(x_1, x_2, x_3), u_3(x_1, x_2, x_3))\end{aligned} \tag{2}$$

is continuous together with its spatial derivatives, the stress components have the form

[a)]Author to whom correspondence should be addressed. Electronic mail: vakorneev@lbl.gov

$$\sigma_{ik} = \lambda \frac{\partial u_s}{\partial x_s}\delta_{ik} + \mu\left(\frac{\partial u_i}{\partial x_k}+\frac{\partial u_k}{\partial x_i}\right)+\left(\mu+\frac{A}{4}\right)\left(\frac{\partial u_s}{\partial x_i}\frac{\partial u_s}{\partial x_k}+\frac{\partial u_k}{\partial x_s}\frac{\partial u_i}{\partial x_s}+\frac{\partial u_s}{\partial x_k}\frac{\partial u_i}{\partial x_s}\right)$$
$$+\frac{(B+\lambda)}{2}\left(\left(\frac{\partial u_s}{\partial x_j}\right)^2\delta_{ik}+2\frac{\partial u_i}{\partial x_k}\frac{\partial u_s}{\partial x_s}\right)+\frac{A}{4}\frac{\partial u_k}{\partial x_s}\frac{\partial u_s}{\partial x_i}+\frac{B}{2}\left(\frac{\partial u_s}{\partial x_j}\frac{\partial u_j}{\partial x_s}\delta_{ik}+2\frac{\partial u_k}{\partial x_i}\frac{\partial u_s}{\partial x_s}\right)+C\left(\frac{\partial u_s}{\partial x_s}\right)^2\delta_{ik}. \quad (3)$$

(Here and below, repeated index s and/or j means summation.)

The equation of motion has the form

$$\rho\frac{\partial^2 u_i}{\partial t^2} = \frac{\partial \sigma_{ik}}{\partial x_k}, \quad (4)$$

or

$$\rho\frac{\partial^2 u_i}{\partial t^2} - \mu\frac{\partial^2 u_i}{\partial x_k^2} - (\lambda+\mu)\frac{\partial^2 u_k}{\partial x_i \partial x_k} = F_i, \quad (5)$$

where F_i, the ith component of a "force" $\mathbf{F}$, is given by

$$F_i = C_1\left(\frac{\partial^2 u_s}{\partial x_k^2}\frac{\partial u_s}{\partial x_i}+\frac{\partial^2 u_s}{\partial x_k^2}\frac{\partial u_i}{\partial x_s}+2\frac{\partial^2 u_i}{\partial x_s \partial x_k}\frac{\partial u_s}{\partial x_k}\right)$$
$$+C_2\left(\frac{\partial^2 u_s}{\partial x_i \partial x_k}\frac{\partial u_s}{\partial x_k}+\frac{\partial^2 u_k}{\partial x_s \partial x_k}\frac{\partial u_i}{\partial x_s}\right)+C_3\frac{\partial^2 u_i}{\partial x_k^2}\frac{\partial u_s}{\partial x_s}$$
$$+C_4\left(\frac{\partial^2 u_k}{\partial x_s \partial x_k}\frac{\partial u_s}{\partial x_i}+\frac{\partial^2 u_s}{\partial x_i \partial x_k}\frac{\partial u_k}{\partial x_s}\right)+C_5\frac{\partial^2 u_k}{\partial x_i \partial x_k}\frac{\partial u_s}{\partial x_s}, \quad (6)$$

and has a second-order value in size.

In Eq. (6), the following notation is used:

$$C_1 = \mu + \frac{A}{4}, \quad C_2 = \lambda+\mu+\frac{A}{4}+B, \quad C_3 = \frac{A}{4}+B,$$
$$C_4 = B+2C, \; C_5 = \lambda + B. \quad (7)$$

Expression (6) for $(i=1,2,3)$ can be converted into a general vector form

$$\mathbf{F} = C_1\mathbf{W_1} + C_2\mathbf{W}_2 + C_3\mathbf{W}_3 + C_4\mathbf{W}_4 + C_5\mathbf{W}_5, \quad (8)$$

where

$$\mathbf{W_1} = [\Delta\mathbf{u}\times\nabla\times\mathbf{u}] + \frac{1}{2}\nabla\Delta(\mathbf{uu}) + \nabla\mathbf{u}\Delta\mathbf{u}$$
$$-\Delta[\mathbf{u}\times\nabla\times\mathbf{u}] + \nabla\times[\mathbf{u}\times\Delta\mathbf{u}] - \mathbf{u}\Delta\nabla\mathbf{u}, \quad (9)$$

$$\mathbf{W}_2 = \frac{1}{2}(\mathbf{W} + \nabla(\nabla\times\nabla\times\mathbf{uu})$$
$$-\nabla[\nabla\nabla\mathbf{u}\times\mathbf{u}] - [\nabla\nabla\mathbf{u}\times\nabla\times\mathbf{u}]), \quad (10)$$

$$\mathbf{W}_3 = \nabla\,\mathbf{u}\Delta\mathbf{u}, \quad (11)$$

$$\mathbf{W}_4 = \frac{1}{2}(\mathbf{W} + [\nabla\nabla\mathbf{u}\times\nabla\times\mathbf{u}]$$
$$-\nabla\times[\nabla\nabla\mathbf{u}\times\mathbf{u}] - \nabla\nabla[\mathbf{u}\times\nabla\times\mathbf{u}]), \quad (12)$$

$$\mathbf{W}_5 = \nabla\mathbf{u}\nabla\nabla\mathbf{u}, \quad (13)$$

$$\mathbf{W} = \frac{1}{2}\nabla\Delta(\mathbf{uu}) - \mathbf{u}\Delta\nabla\mathbf{u} + \nabla\mathbf{u}\nabla\nabla\mathbf{u}, \quad (14)$$

which is ready to use in systems other than Cartesian coordinate system. For most solids, the values of the nonlinear constants (A, B, C) are significantly larger than those of constants λ and μ, which may be neglected in the nonlinear parts of wave solutions.

III. NONLINEAR INTERACTION OF ELASTIC WAVES

Under some circumstances, elastic waves with different frequencies ω_1 and ω_2 propagating in a solid may interact and produce secondary waves of mixed (sum or difference) frequencies ω_g. Theoretically, this problem is similar to phonon-phonon interactions, a subject of quantum mechanics. The conditions for such resonant interactions existing are

$$\omega_g = \omega_1 \pm \omega_2, \quad (15a)$$

$$\mathbf{k}_g = \mathbf{k}_1 \pm \mathbf{k}_2, \quad (15b)$$

where (15b) includes the corresponding wave vectors. The "plus" sign in (15) corresponds to the case of sum resonant frequencies; the "minus" sign corresponds to the case of difference resonant frequencies. Therefore, condition (15a) defines the frequencies of scattered waves, while condition (15b) defines their direction of propagation. In the case of a liquid medium without dispersion, condition (15b) means that interaction is possible for collinear waves only. For solids, because of the existence of two velocities of propagation, a variety of different resonance interactions become possible. The geometries of sum and difference resonance interactions are illustrated in Fig. 1. The interaction angle α is a solution of the equation

$$\left(\frac{\omega_g}{v_g}\right)^2 = \left(\frac{\omega_1}{v_1}\right)^2 + \left(\frac{\omega_2}{v_2}\right)^2 \pm 2\frac{\omega_1}{v_1}\frac{\omega_2}{v_2}\cos\alpha, \quad (16)$$

which is the result of (15b). Velocities v_1, v_2, v_g might be equal to either v_L or v_S, depending on the types of interaction, where propagation velocities

$$v_L = \sqrt{\frac{\lambda+2\mu}{\rho}} \quad \text{and} \quad v_S = \sqrt{\frac{\mu}{\rho}} \quad (17)$$

correspondingly relate to longitudinal and shear waves in an elastic medium with material density ρ.

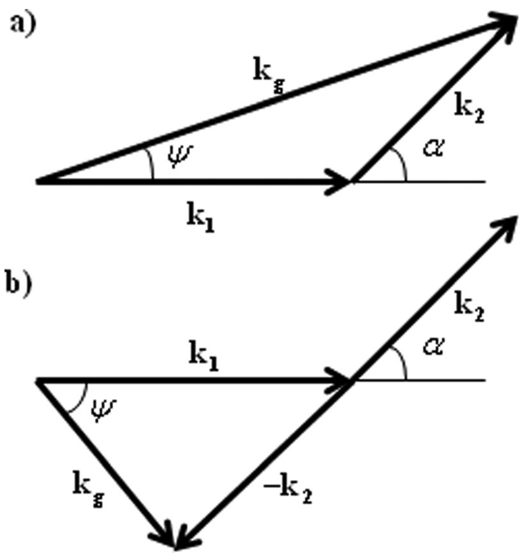

FIG. 1. Angle definitions for (a) sum and (b) difference frequency generation.

The two equations in Eq. (15), together with conditions,

$$-1 \leq \cos\alpha \leq 1 \tag{18}$$

might not be satisfied for some combinations of waves and frequencies, which means that certain types of interactions cannot exist.

The propagation angle ψ of the resonant wave is defined by geometry in Fig. 1 and can be found from the following equation:

$$\mathrm{tg}\,\psi = \frac{\pm\frac{v_1}{v_2} d \sin\alpha}{1 \pm \frac{v_1}{v_2} d \cos\alpha}, \tag{19}$$

where

$$d = \frac{\omega_2}{\omega_1}. \tag{20}$$

Basic expressions for the interaction of elastic waves in an isotropic solid were obtained by Jones and Kobett,[22] Taylor and Rollins,[23] and Zarembo and Krasil'nikov.[11] They considered the sum of two incident plane waves

$$\mathbf{u}_0 = A_1 \cos(\omega_1 t - \mathbf{k}_1\mathbf{r})\mathbf{a}_1 + A_2 \cos(\omega_2 t - \mathbf{k}_2\mathbf{r})\mathbf{a}_2 \tag{21}$$

with amplitudes A_j and polarizations $\mathbf{a}_j$ $(j = 1, 2)$, which are substituted into the equation of motion (5). Polarization vectors $\mathbf{a}_j$ are parallel to wave-number vectors $\mathbf{k}_j$ for L-waves and orthogonal to them for S waves. S-waves with components polarized in the interaction plane will be referred as SV, while shear waves with polarization orthogonal to this plane will be referred as SH. Denoting by $\mathbf{p}$ that part of $\mathbf{F}$ from Eq. (6) which describes the interaction of waves, it can be written in the form

$$\mathbf{p}(r,t) = -A_1A_2\big(\mathbf{I}^{+}\sin[(\omega_1+\omega_2)t - (\mathbf{k}_1+\mathbf{k}_2)\mathbf{r})] + \mathbf{I}^{-}\sin[(\omega_1-\omega_2)t - (\mathbf{k}_1-\mathbf{k}_2)\mathbf{r})]\big), \tag{22}$$

where

$$\begin{aligned}\mathbf{I}^{\pm} = {} & \frac{1}{2}C_1\big[(\mathbf{a}_1\mathbf{a}_2)(k_2^2\mathbf{k}_1 \pm k_1^2\mathbf{k}_2) + (\mathbf{a}_2\mathbf{k}_1)k_2(k_2 \pm 2k_1\cos\alpha)\mathbf{a}_1 + (\mathbf{a}_1\mathbf{k}_2)k_1(2k_2\cos\alpha \pm k_1)\mathbf{a}_2\big]\\ & + \frac{1}{2}C_2 k_1k_2\cos\alpha[(\mathbf{a}_1\mathbf{a}_2)(\mathbf{k}_2 \pm \mathbf{k}_1) + (\mathbf{a}_2\mathbf{k}_2)\mathbf{a}_1 \pm (\mathbf{a}_1\mathbf{k}_1)\mathbf{a}_2]\\ & + \frac{1}{2}C_3[(\mathbf{a}_1\mathbf{k}_2)((\mathbf{a}_2\mathbf{k}_2) \pm (\mathbf{a}_2\mathbf{k}_1))\mathbf{k}_1 + (\mathbf{a}_2\mathbf{k}_1)((\mathbf{a}_1\mathbf{k}_2) \pm (\mathbf{a}_1\mathbf{k}_1))\mathbf{k}_2]\\ & + \frac{1}{2}C_4(\mathbf{a}_2\mathbf{k}_2)[(\mathbf{a}_1\mathbf{k}_2)\mathbf{k}_2 \pm (\mathbf{a}_1\mathbf{k}_1)\mathbf{k}_1] + \frac{1}{2}C_5\big[(\mathbf{a}_1\mathbf{k}_1)k_2^2\mathbf{a}_2 \pm (\mathbf{a}_2\mathbf{k}_2)k_1^2\mathbf{a}_1\big].\end{aligned} \tag{23}$$

Expressions of the forms $(\mathbf{xy})$ in Eq. (23) and later denote scalar products.

If there is a volume V inside the medium where the primary beams are well collimated and if it is assumed that waves interact only in this volume, it is possible to obtain a solution for the scattered secondary field in the far field,

$$\mathbf{u_1}(r,t) = \frac{A_1A_2}{4\pi r\rho}\sum_{\xi=+,-}\left(\frac{(\mathbf{I}^{\xi}\hat{\mathbf{r}})\hat{\mathbf{r}}}{v_L^2}V_L^{\xi} + \frac{\mathbf{I}^{\xi} - (\mathbf{I}^{\xi}\hat{\mathbf{r}})\hat{\mathbf{r}}}{v_S^2}V_S^{\xi}\right), \tag{24}$$

where $\mathbf{r} = r\hat{\mathbf{r}}$ $|\hat{\mathbf{r}}| = 1$, is the radius vector from the center point of the interaction region and observation point. Here and later, $\xi =$"+" indicates the sum frequency, and $\xi =$"−" indicates the difference frequency interactions.

Integrals

$$V_g^{\pm} = \int_V \sin\left(\Delta_g^{\pm} - \left(\mathbf{k}_1 \pm \mathbf{k}_2 - \frac{\omega_1 \pm \omega_2}{v_g}\hat{\mathbf{r}}\right)\mathbf{r}'\right)dV \tag{25}$$

from Eq. (24) are referred to as volume factors, and

$$\Delta_g^{\pm} = (\omega_1 \pm \omega_2)\left(\frac{r}{v_g} - t\right) \tag{26}$$

is the scattering phase. In Eq. (25) $\mathbf{r}'$ is the radius vector of integration inside the volume V (geometry shown in Fig. 2). Symbol g can be either "L" or "S," denoting the type of scattered wave.

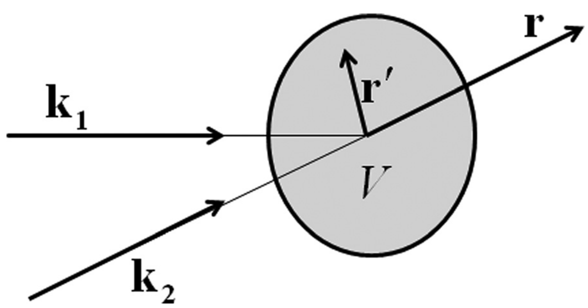

FIG. 2. Interaction of two plane waves in a volume V of a nonlinear elastic material.

Equation (24) has four terms corresponding to both sum and difference frequencies for L and S waves. As we integrate over dV, the integrand in Eq. (25) oscillates with frequencies determined by the coefficients of $\mathbf{r}'$, and the results of any integration will depend on just how the waves fit into the region V. Scattered waves have natural polarizations: Parallel to $\mathbf{r}$ for L- waves and orthogonal to $\mathbf{r}$ for S-waves.

If we satisfy resonant conditions (15) by choosing an appropriate direction $\hat{\mathbf{r}} = \hat{\mathbf{r}}_g$, the corresponding coefficient of $\mathbf{r}'$ in (25) becomes equal to zero, and the amplitude of the scattered wave in this direction becomes proportional to the volume V of integration. From (24), it also follows that amplitudes of the scattered waves are proportional to their projections in the direction $\mathbf{a}_g^\xi$, which is the unit vector of the natural polarization of the wave. For L-waves, $\mathbf{a}_g^\xi$ is parallel to $\hat{\mathbf{r}}_g$; for S-waves, it is perpendicular to this vector. That means that the resonant scattering amplitude may be zero even if resonant conditions (15) are satisfied. A zero value of the scattering amplitude due to polarization will be referred to as *polarization restriction*.

All types of elastic-wave resonant interactions are listed in Table I, where signs "x" and "x̄" signify that interaction is possible, and sign "=" signifies that interaction is possible only when interacting waves are collinear. Sign "x̄" indicates that interaction is also possible when waves propagate antilinearly (in opposite directions). All other types of interactions are forbidden. Sign "O" marks interactions that are forbidden because of polarization restrictions; all others are forbidden because the resonant conditions (23) for them cannot be satisfied. Only 10 out of 54 potential interactions are possible. Sum frequency resonance exists only for compressional scattered waves. Sum frequency interactions for L + SV- > L and SV + L- > L combinations are reciprocal.

TABLE I. Forbidden and allowed scattering processes for an isotropic solid: "="—possible only when waves are collinear (propagate in one direction); "x" and "x̄"—scattering possible for certain range of parameters, where "x̄" also means that antilinear interaction is possible (waves propagate in opposite directions); "O"—polarization restriction, blank space—interaction restriction.

		Scattered waves					
		$\omega_r = \omega_1 + \omega_2$			$\omega_r = \omega_1 - \omega_2$		
N	Interaction waves	L	SV	SH	L	SV	SH
1	L(ω_1) and L(ω_2)	=			=	x̄	O
2	L(ω_1) and SV(ω_2)	x̄			x	x̄	O
3	SV(ω_1) and L(ω_2)	x					
4	SV(ω_1) and SV(ω_2)	x̄	O	O		O	O
5	SH(ω_1) and SH(ω_2)	x̄	O	O		O	O
6	L(ω_1) and SH(ω_2)	O			O	O	x̄
7	SH(ω_1) and L(ω_2)	O					
8	SH(ω_1) and SV(ω_2)	O	O	O		O	O
9	SV(ω_1) and SH(ω_2)	O	O	O		O	O

A similar table of allowed and forbidden scattering processes for an isotropic solid published in the Zarembo and Krasil'nikov[11] contains 18 possible interactions. We believe their results are partly in error. Taylor and Rollins[23] have presented five possible interactions, omitting the problem of separation of SV and SH polarization for shear waves. Childress and Hambrick[24] present eight interactions, while Holt and Ford[25] found ten interactions by numerical search using parameters for copper.

If resonant conditions (15) are satisfied for any one type of interaction, the scattered field from (24) may be rewritten in the form

$$\mathbf{u_1}(r,t) = \mathbf{a}_g^\xi W_g^\xi \frac{A_1 A_2}{r} V_g^\xi, \tag{27}$$

with amplitude coefficient

$$W_g^\xi = \frac{(\mathbf{I}^\xi \mathbf{a}_g^\xi)}{4\pi v_g^2 \rho}. \tag{28}$$

From (28), it is seen that the scattering amplitude is proportional to the coefficient W_g^ξ with dimension *length*$^{-3}$ and to the scattering volume V_g^ξ, so the product of these quantities is dimensionless.

Analytical expressions for W_g^ξ of all ten possible scattering interactions are listed in Table II together with expressions for interacting angle, α and limits, $d_{\min}$, $d_{\max}$, of the frequency ratio d. In addition, the following notations are used:

$$D_g = \frac{d}{4\pi(\lambda + 2\mu)} \left(\frac{\omega_1}{v_g}\right)^3, \quad \gamma = \sqrt{\frac{\mu}{\lambda + 2\mu}} = \frac{v_S}{v_P}. \tag{29}$$

Approximate expressions for scattering amplitudes in Table II are derived from exact formulas, under the assumption that in coefficients (7) we may neglect Lamé constants for components containing nonlinear TOE constants. These expressions were verified by comparison with numerical solutions for Eqs. (23) and (28). Note, that the Lamé constants are involved in the approximate W_g^ξ expressions via coefficient D_g [Eq. (29)].

IV. SCATTERING BEAMWIDTH

The scattered waves, given by (24), appear in the form of conical beams with vertexes at the interaction zone and maximum intensity in the direction $\hat{\mathbf{r}}_g$. To investigate the amplitudes of the scattering beams as a function of observation position, it is convenient to assume that the interaction volume has the shape of a sphere of radius R. Any volume factor from (25) may then be reduced to the form

$$V_g^\pm = \Delta_g^\pm \int_V \sin a(\hat{\mathbf{r}}\mathbf{r}')dV = 3V \frac{j_1(aR)}{aR} \Delta_g^\pm, \tag{30}$$

$$a = \left| \mathbf{k}_1 \pm \mathbf{k}_2 - \frac{\omega_1 \pm \omega_2}{v_g} \hat{\mathbf{r}} \right|, \tag{31}$$

TABLE II. Nonlinear scattering coefficients of two plane elastic wave interaction.

#	Interaction	$\cos\alpha$	$d_{\min}$	$d_{\max}$	Scattering coefficient
1	$L(\omega_1)+L(\omega_2)$ $\rightarrow L(\omega_1+\omega_2)$	1	0	∞	$D_L\frac{1+d}{2}(4C_1+2C_2+2C_3+C_4+C_5)\approx D_L(1+d)(2m+l)$
2	$L(\omega_1)+L(\omega_2)$ $\rightarrow L(\omega_1-\omega_2)$	1	0	1	$-D_L\frac{1-d}{2}(4C_1+2C_2+2C_3+C_4+C_5)\approx -D_L(1-d)(2m+l)$
3	$L(\omega_1)+L(\omega_2)$ $\rightarrow SV(\omega_1-\omega_2)$	$\frac{1}{\gamma^2}-\frac{1}{2}\left(d+\frac{1}{d}\right)\left(\frac{1}{\gamma^2}-1\right)$	$\frac{1-\gamma}{1+\gamma}$	1	$-D_S\frac{1+d}{4}\gamma^2\sin 2\alpha(2C_1+C_2+C_3)\approx -D_S(1+d)\gamma^2 m\sin 2\alpha/2$
4	$L(\omega_1)+SV(\omega_2)$ $\rightarrow L(\omega_1+\omega_2)$	$\gamma-\frac{d}{2}\left(\frac{1}{\gamma}-\gamma\right)$	0	$\frac{2\gamma}{1-\gamma}$	$-\frac{D_L}{2\gamma^3}\frac{\sin\alpha}{1+d}[C_1(3d\gamma+2q)+C_2q+C_3(d\gamma+q)+d\gamma C_5]$ $\approx -\frac{D_L}{\gamma^3}\frac{\sin\alpha}{1+d}(d\gamma+q)m$ $q=\cos\alpha(2d\gamma\cos\alpha+d^2+2\gamma^2)$
5	$L(\omega_1)+SV(\omega_2)$ $\rightarrow L(\omega_1-\omega_2)$	$\gamma+\frac{d}{2}\left(\frac{1}{\gamma}-\gamma\right)$	0	$\frac{2\gamma}{1+\gamma}$	$-\frac{D_L}{2\gamma^3}\frac{\sin\alpha}{1-d}[C_1(3d\gamma+2q)+C_2q+C_3(d\gamma+q)+d\gamma C_5]$ $\approx -\frac{D_L}{\gamma^3}\frac{\sin\alpha}{1-d}(d\gamma+q)m,\ q=-\cos\alpha(2-2d+d^2)$
6	$L(\omega_1)+SV(\omega_2)$ $\rightarrow SV(\omega_1-\omega_2)$	$\frac{1}{\gamma}-\frac{1}{2d}\left(\frac{1}{\gamma}-\gamma\right)$	$\frac{1-\gamma}{2}$	$\frac{1+\gamma}{2}$	$\frac{D_S}{2\gamma^3(1-d)}[C_1(2qd-\gamma^2\cos 2\alpha+\gamma d\cos\alpha)-C_2q\gamma\cos\alpha+C_3\gamma^2\sin^2\alpha+C_5dq]$ $\approx\frac{D_S}{2\gamma^3}\frac{m}{1-d}(2d\gamma\cos\alpha-d^2-\gamma^2\cos 2\alpha)$ $q=\gamma\cos\alpha-d$
7	$SV(\omega_1)+L(\omega_2)$ $\rightarrow L(\omega_1+\omega_2)$	$\gamma-\frac{1}{2d}\left(\frac{1}{\gamma}-\gamma\right)$	$\frac{1-\gamma}{2\gamma}$	∞	$\frac{D_L}{2\gamma^3}\frac{\sin\alpha}{1+d}[C_1(3d\gamma+2q)+C_2q+C_3(d\gamma+q)+d\gamma C_5]$ $\approx\frac{D_L}{\gamma^3}\frac{\sin\alpha}{1+d}(d\gamma+q)m,$ $q=\cos\alpha(2d\gamma\cos\alpha+1+2\gamma^2d^2)$
8	$SV(\omega_1)+SV(\omega_2)$ $\rightarrow L(\omega_1+\omega_2)$	$\gamma^2+\frac{1}{2}\left(d+\frac{1}{d}\right)(\gamma^2-1)$	$\frac{1-\gamma}{1+\gamma}$	$\frac{1+\gamma}{1-\gamma}$	$D_L\frac{1+d}{2\gamma^2}(C_1\cos 2\alpha+C_2\cos^2\alpha-C_3\sin^2\alpha)\approx D_L\frac{1+d}{2\gamma^2}m\cos 2\alpha$
9	$SH(\omega_1)+SH(\omega_2)$ $\rightarrow L(\omega_1+\omega_2)$	$\gamma^2+\frac{1}{2}\left(d+\frac{1}{d}\right)(\gamma^2-1)$	$\frac{1-\gamma}{1+\gamma}$	$\frac{1+\gamma}{1-\gamma}$	$\frac{D_L}{2\gamma^4(1+d)}[C_1(2d+\cos\alpha(1+d^2))+C_2\gamma^2\cos\alpha(1+d)^2]$ $\approx\frac{D_L}{2\gamma^4(1+d)}[m\gamma^2\cos\alpha(1+d)^2+$ $n(2d+\cos\alpha(1+d^2-\gamma^2(1+d)^2))/4]$
10	$L(\omega_1)+SH(\omega_2)$ $\rightarrow SH(\omega_1-\omega_2)$	$\frac{1}{\gamma}-\frac{1}{2d}\left(\frac{1}{\gamma}-\gamma\right)$	$\frac{1-\gamma}{2}$	$\frac{1+\gamma}{2}$	$\frac{D_S}{2\gamma}[C_1\cos\alpha(2d\cos\alpha-\gamma)-C_2\gamma\cos\alpha+C_5d]$ $\approx D_S\left[2m(d-\gamma\cos\alpha)-nd\sin^2\alpha\right]/(4\gamma)$

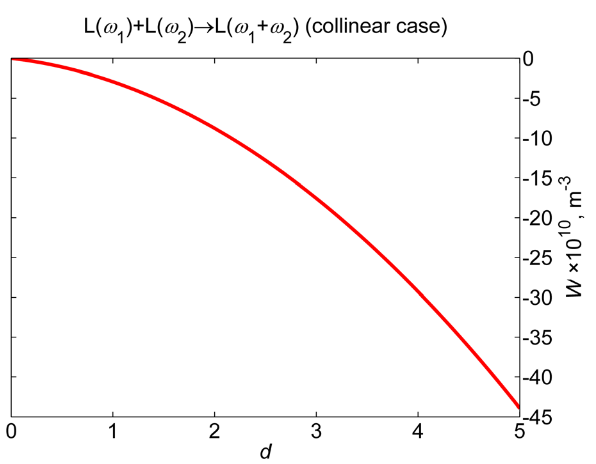

FIG. 3. (Color online) Interaction $L(\omega_1)+L(\omega_2)\rightarrow L(\omega_1+\omega_2)$.

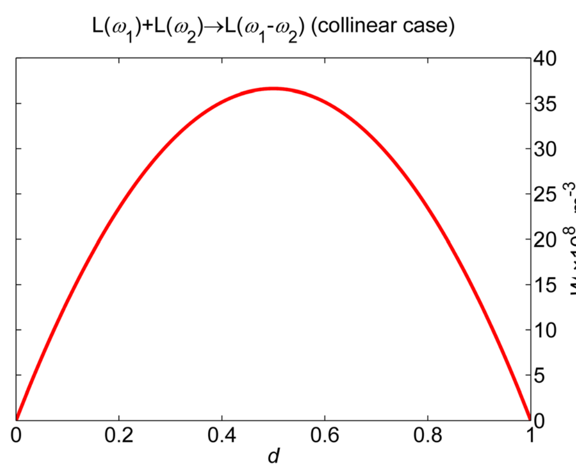

FIG. 4. (Color online) Interaction $L(\omega_1)+L(\omega_2)\rightarrow L(\omega_1-\omega_2)$.

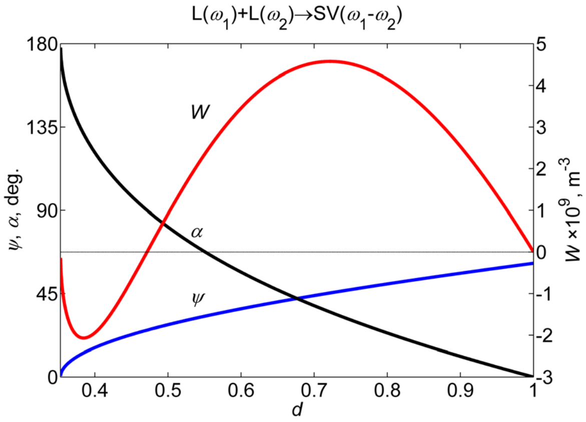

FIG. 5. (Color online) Interaction $L(\omega_1) + L(\omega_2) \to SV(\omega_1 - \omega_2)$.

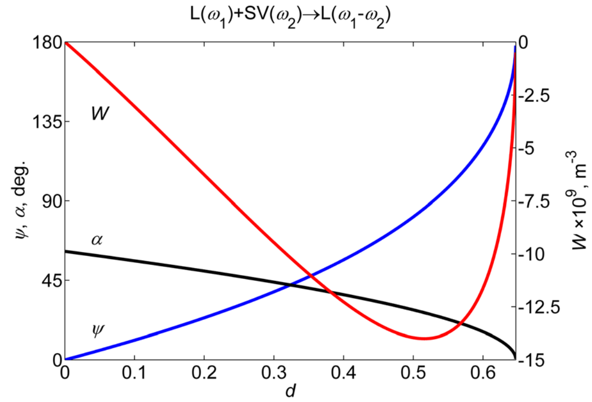

FIG. 7. (Color online) Interaction $L(\omega_1) + SV(\omega_2) \to L(\omega_1 - \omega_2)$.

where $V = (4\pi/3)R^3$ is the volume of the sphere, $j_1(x)$ is the spherical Bessel function of the first order.

If θ is the angle between resonant scattering direction $\hat{\mathbf{r}}_g$, and observation direction $\hat{\mathbf{r}}$, we obtain

$$aR = 2\pi \frac{R}{\lambda_g} \sqrt{2(1 - \cos\theta)}, \tag{32}$$

where λ_g is the wavelength of the scattered wave. Assuming the interaction volume is spherical, this analysis shows that the volume factor is proportional to the volume of the sphere. Using the asymptotic approximation for spherical Bessel functions in (30), we may estimate the total beamwidth θ_w of the scattering beam, where the amplitude of the scattering beam is not less than one half of its maximum. The result is

$$\theta_w \approx 2 \arccos\left(1 - \frac{1}{10}\left(\frac{\lambda_g}{R}\right)^2\right). \tag{33}$$

For small angles ($\theta_w < 0.1$) (33) reduces to

$$\theta_w \approx \frac{\lambda_g}{R}. \tag{34}$$

V. NUMERICAL RESULTS

Equations from Table II allow computation of the interaction angle, scattering angle, and scattering coefficient for any set of elastic parameters. Here we apply a set of parameters for polyvinyl chloride (PVC), as follows: $\lambda = 3.64$ GPa, $\mu = 1.83$ GPa, $l = -33.43$ GPa, $m = -20.88$ GPa, $n = -15.86$ GPa, and $\rho = 1350$ kg/m^3. The third-order elastic constants are measured using an acousto-elastic measurement method. Amplitude coefficients W_g^ξ as well as interaction α and scattering γ angles for all possible (ten) interactions from Tables I and II, are shown in Figs. 3–12 as functions of the frequency ratio $d = \omega_2/\omega_1$. The calculations are performed when $\omega_1 = 2\pi \times 1$ MHz.

VI. DISCUSSION AND CONCLUSIONS

We confirm the possibility of just ten interactions for nonlinear wave mixing, as listed in Table I. Sum frequency interactions #4 for L + SV- > L and #7 SV + L- > L combinations are reciprocal. Indeed, if in an expression for scattering coefficient for interaction #7 (Table II), we exchange parameter d for $1/d$ and reverse the sign for angle α, then the result is identical to that for interaction #4.

The results in Table II reveal a rather simple dependence of scattering amplitudes on nonlinear elastic constants. Amplitudes of two collinear LL interactions are proportional to $2m + l$, while six interactions are proportional to m and independent of other constants. The remaining two interactions, in which SH waves are involved, have more complicated dependence on constants m and n. Note that some frequency-ratio values cause zeroes for interaction coefficients, but this is an easily avoidable problem for nonlinear wave experiments. These zeroes, if detected, can be the extra constraints for determining model parameters.

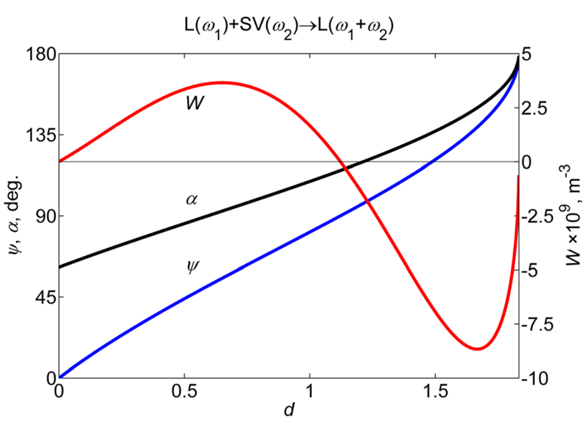

FIG. 6. (Color online) Interaction $L(\omega_1) + SV(\omega_2) \to L(\omega_1 + \omega_2)$.

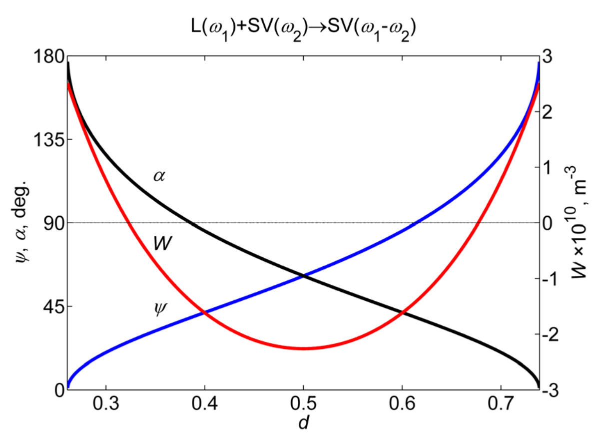

FIG. 8. (Color online) Interaction $L(\omega_1) + SV(\omega_2) \to SV(\omega_1 - \omega_2)$.

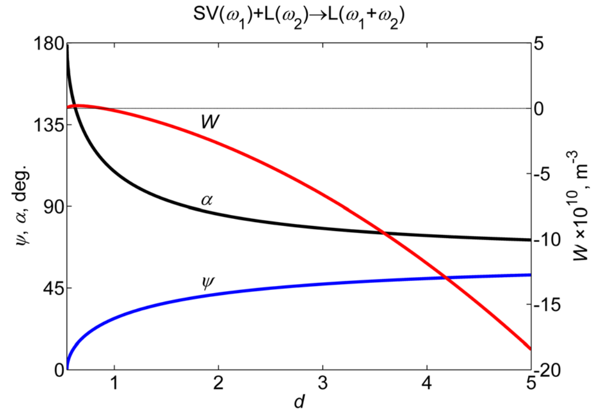

FIG. 9. (Color online) Interaction $SV(\omega_1)+L(\omega_2)\to L(\omega_1+\omega_2)$.

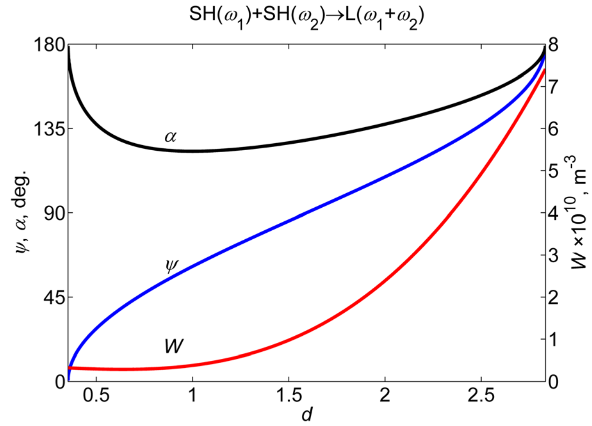

FIG. 11. (Color online) Interaction $SH(\omega_1)+SH(\omega_2)\to L(\omega_1+\omega_2)$.

Depending on the geometry of a sample, available sources, and nonlinear parameters of interest, an appropriate interaction should be chosen for reaching the largest possible amplitude of the resonant wave. Not only is this amplitude proportional to both amplitudes A_j $(j=1,2)$ of the primary waves, it is also proportional to the coefficients W_g^ξ and the scattering volume V_g^ξ. Generally, the sum frequency interactions have higher amplitudes than those with difference frequencies.

A special interest might represent reactions marked by $\bar{x}$ in Table I, when the primary waves propagate in exactly opposite directions. A laboratory setup for such a situation might be preferable because in this case computation of interaction angles is not needed.

The approximate expressions in Table II are derived in assumption that TOE constants are much larger than Lame constants, which may be neglected in Eq. (7). This assumption is supported by a number of measurements for a variety of materials.[11,26–29] It should be noticed that in many publications, for evaluations of TOE constants were used the equations from Jones and Kobett (1963), which apparently have some errors in them.[30] These errors are likely affected the values of some of the published TOE constants, although not affecting their orders of magnitude.

Different nature of restrictions on interaction types from Table I suggests that in some circumstances some of the restrictions can vanish. Thus, the polarization restriction can vanish in anisotropic medium where wave vectors and polarization vectors are not perfectly collinear (orthogonal). Also, in such a medium the interaction restriction between two shear waves might disappear because of different velocities of those waves.

Determination of the interaction volume is generally an important issue because the actual objects of study might have a complex shape and finite sizes when an assumption about an infinite nonlinear material is invalid. We considered a spherical interaction volume because this case allows an analytical solution. In practical applications (e.g., nonlinear scanning), the shape of the material sample can be arbitrary and the interaction volume can be evaluated by a numerical computation of integrals (25). For simple shapes, this computation should be performed just once because of repeating geometry. We also assumed that the interaction volume has nonzero TOE constants while the other material parameters in that volume have the same values as in the surrounding medium. In a general case when all the parameters change, a correspondent linear diffraction problem should be involved. Thus, for a spherical geometry, a linear canonical diffraction problem can be solved using spherical harmonics,[31] and then used for evaluating of the nonlinear part. Equations (8)–(14) can be simply converted into the spherical coordinate system for this purpose. Consideration of such general case is beyond the scope of this paper. The results obtained here were applied for measurements of plastic ageing and epoxy

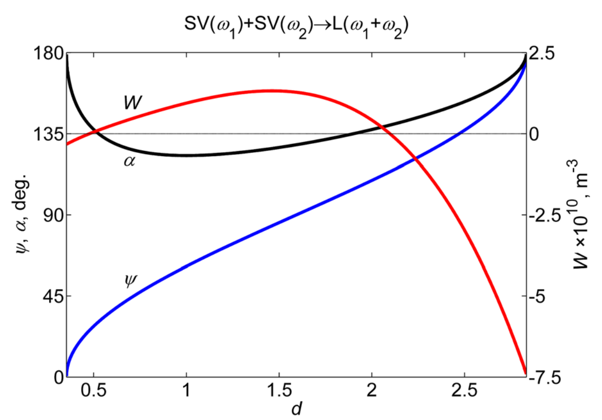

FIG. 10. (Color online) Interaction $SV(\omega_1)+SV(\omega_2)\to L(\omega_1+\omega_2)$.

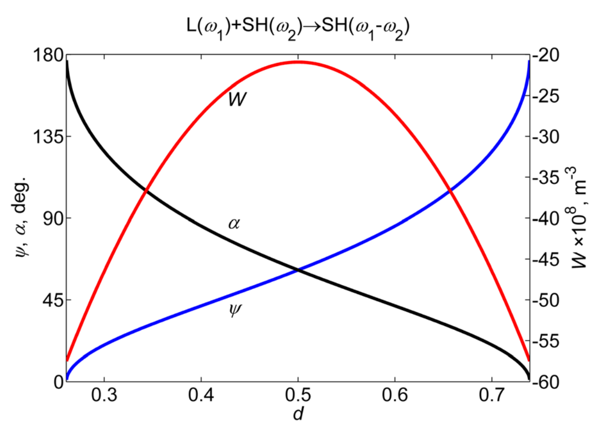

FIG. 12. (Color online) Interaction $L(\omega_1)+SH(\omega_2)\to SH(\omega_1-\omega_2)$.

curing and published in Demčenko *et al.*[32] using an immersion method with a thorough discussion on the optimal choice of laboratory parameters. In particular, some of these measurements revealed that the observed changes indeed can appear just in the nonlinear part of the field when the linear part remain insensitive to the changes.

The immersion method does not require a direct contact between the measuring hardware and a specimen which allows scanning and/or monitoring of nonlinear properties. Nonlinear wave mixing in this application is likely to become a routine non-destructive testing technique.

ACKNOWLEDGMENTS

This work was supported by the Director, Office of Energy Research, Office of Basic Energy Sciences, Engineering and Geosciences Division, of the U.S. Department of Energy under Contract No. DE-ACO2-05CH11231. This work was also carried out in partial collaboration with Vitens and Applus RTD within the "Innowator" project IWA-08019, as funded by the Dutch Ministry of Economic Affairs, by means of Agentschap NL. Tania Vulfs helped to verify some analytical results from Table II.

[1] M. A. Breazeale and D. O. Thompson, "Finite-amplitude ultrasonic waves in aluminum," Appl. Phys. Lett. **3**, 77–78 (1963).
[2] P. H. Carr, "Harmonic generation of microwave phonons in quartz," Phys. Rev. Lett. **13**, 332–335 (1964).
[3] P. H. Carr, "Harmonic generation of microwave phonons by radiation pressure and by the phonon-phonon interaction," IEEE T. Son. Ultrason. **13**, 103–108 (1966).
[4] K. K. Ermilin, L. K. Zarembo, and V. A. Krasil'nikov, "Generation of superhigh frequency acoustic harmonics in a lithium niobate crystals," Sov. Phys. Solid State **12**, 1045–1052 (1970).
[5] A. A. Gedroits and V. A. Krasil'nikov, "Finite-amplitude elastic waves amplitude in solids and deviations from the Hooke's law," JETP Lett. **16**, 1122 (1963).
[6] N. S. Shiren, "Nonlinear acoustic interaction in MgO at 9 Gc/sec," Phys. Rev. Lett. **11**, 3–6 (1963).
[7] A. Hikata, B. B. Chick, and C. Elbaum, "Dislocation contribution to the second harmonic generation of ultrasonic waves," J. Appl. Phys. **36**, 229–236 (1965).
[8] P. A. Johnson and K. R. McCall, "Observation and implications of nonlinear elastic wave response in rock," Geophys. Res. Lett. **21**, 165–168, doi:10.1029/93GL03162 (1994).
[9] Y. Hiki and K. Mukai, "Ultrasonic three-phonon process in copper crystal," J. Phys. Soc. Jpn. **34**, 454–461 (1973).
[10] F. R. Rollins, L. H. Taylor, and P. H. Todd, "Ultrasonic study of three-phonon interactions. II. Experimental results," Phys. Rev. **136**, A597–A601 (1964).
[11] L. K. Zarembo and V. A. Krasil'nikov, "Nonlinear phenomena in the propagation of elastic waves in solids," Sov. Phys. Usp. **13**, 778–797 (1971).
[12] P. A. Johnson, T. J. Shankland, R. J. O'Connell, and J. N. Albright, "Nonlinear generation of elastic waves in crystalline rock," J. Geophys. Res. **92**, 3597–3602, doi:10.1029/JB092iB05p03597 (1987).
[13] P. A. Johnson and T. J. Shankland, "Nonlinear generation of elastic waves in granite and sandstone: Continuous wave and travel time observations," J. Geophys. Res. **94**, 17 729–17 733, doi:10.1029/JB094iB12p17729 (1989).
[14] H. H. Barrett and J. H. Matsinger, "Interaction of almost-collinear longitudinal phonons," Phys. Rev. **154**, 877–886 (1967).
[15] R. W. Dunham and H. B. Huntington, "Ultrasonic beam mixing as a measure of the nonlinear parameters of fused silica and single-crystal NaCl," Phys. Rev. B **2**, 1098–1107 (1970).
[16] A. J. Croxford, P. D. Wilcox, B. W. Drinkwater, and P. B. Nagy, "The use of non-collinear mixing for nonlinear ultrasonic detection of plasticity and fatigue," J. Acoust. Soc. Am. **126**, EL117–EL122 (2009).
[17] A. Demčenko, R. Akkerman, P. B. Nagy, and R. Loendersloot, "Non-collinear wave mixing for non-linear ultrasonic detection of physical ageing in PVC," NDT & E Int. **49**, 34–39 (2012).
[18] F. D. Murnaghan, *Finite Deformation of an Elastic Solid* (John Wiley & Sons, New York, 1951), 140 pp.
[19] L. K. Zarembo and V. A. Krasil'nikov, *Introduction in Nonlinear Acoustics* (Science, Moscow, 1966), Chap. 8 (in Russian).
[20] V. A. Korneev, K. T. Nihei, and L. R. Myer, "Nonlinear interaction of plane elastic waves," Tech. Rep. LBNL-41914 (Lawrence Berkeley National Laboratory, Berkeley, CA, 1998).
[21] L. D. Landau and E. M. Lifshitz, *Theory of Elasticity* (Pergamon Press, New York, 1959), 134 pp.
[22] G. L. Jones and D. R. Kobett, "Interaction of elastic waves in an isotropic solid," J. Acoust. Soc. Am. **35**, 5–10 (1963).
[23] L. H. Taylor and F. R. Rollins, "Ultrasonic study of three-phonon interactions. I. Theory," Phys. Rev. **136**, A591–A596 (1964).
[24] J. D. Childress and C. G. Hambrick, "Interactions between elastic waves in an isotropic solid," Phys. Rev. **136**, A411–A418 (1964).
[25] A. C. Holt and J. Ford, "Theory of ultrasonic three-phonon interactions in single-crystal solids," J. Appl. Phys. **40**, 142–148 (1969).
[26] P. A. Johnson and P. N. J. Rasolofosaon, "Nonlinear elasticity and stress-induced anisotropy in rock," J. Geophys. Res. **101**, 3113–3124, doi:10.1029/95JB02880 (1996).
[27] V. E. Nazarov, L. A. Ostrovsky, I. A. Soustova, and A. M. Sutin, "Nonlinear acoustics of micro-inhomogeneous media," Phys. Earth Planet. Inter. **50**, 65–73 (1988).
[28] R. Prioul, A. Bakulin, and V. Bakulin, "Nonlinear rock physics model for estimation of 3D subsurface stress in anisotropic formations: Theory and laboratory verification," Geophysics **69**, 415–425 (2004).
[29] D. Sarkar, A. Bakulin, and R. L. Kranz, "Anisotropic inversion of seismic data for stressed media: Theory and a physical modeling study on Berea sandstone," Geophysics **68**, 690–704 (2003).
[30] V. Korneev and S. Glubokovskikh, "Seismic velocity changes caused by an overburden stress," Geophysics **78**, WC25–WC31 (2013).
[31] V. A. Korneev and L. R. Johnson, "Scattering of P and S waves by spherically symmetric inclusion," Pure Appl. Geophys. **147**, 675–718 (1996).
[32] A. Demčenko, V. Koissin, and V. A. Korneev, "Noncollinear wave mixing for measurement of dynamic processes in polymers: Physical ageing in thermoplastics and epoxy cure," Ultrasonics **54**, 684–693 (2014).